A Field-Based Approach for Determining ATOFMS Instrument Sensitivities to Ammonium and Nitrate

PRAKASH V. BHAVE

Department of Environment Science and Engineering, California Institute of Technology, Pasadena, California 91125-7800

JONATHAN O. ALLEN

Departments of Chemical & Materials Engineering and Civil & Environmental Engineering, Arizona State University, Tempe, Arizona 82876-6006

BRADLEY D. MORRICAL[†] AND DAVID P. FERGENSON[‡]

Department of Chemistry, University of California, Riverside, Riverside, California 92521

GLEN R. CASS[§]

School of Earth and Atmospheric Sciences, Georgia Institute of Technology, Atlanta, Georgia 39332-0340

KIMBERLY A. PRATHER*

Department of Chemistry and Biochemistry, University of California, San Diego, La Jolla, California 92093-0314

Aerosol time-of-flight mass spectrometry (ATOFMS) instruments measure the size and chemical composition of individual particles in real-time. ATOFMS chemical composition measurements are difficult to quantify, largely because the instrument sensitivities to different chemical species in mixed ambient aerosols are unknown. In this paper, we develop a field-based approach for determining ATOFMS instrument sensitivities to ammonium and nitrate in size-segregated atmospheric aerosols, using tandem ATOFMS-impactor sampling. ATOFMS measurements are compared with collocated impactor measurements taken at Riverside, CA, in September 1996, August 1997, and October 1997. This is the first comparison of ion signal intensities from a single-particle instrument with quantitative measurements of atmospheric aerosol chemical composition. The comparison reveals that ATOFMS instrument sensitivities to both NH_4^+ and NO_3^- decline with increasing particle aerodynamic diameter over a 0.32–1.8 μm calibration range. The stability of this particle size dependence is tested over the broad range of fine particle concentrations ($PM_{1.8} = 17.6 \pm 2.0$–127.8 ± 1.8 μg m^{-3}), ambient temperatures (23–35 °C), and relative humidity conditions (21–

* Corresponding author phone: (858)822-5312; fax: (858)534-7042; e-mail: kprather@ucsd.edu.

† Present address: Laboratory of Organic Chemistry, ETH Hönggerburg, HCI E330, 8093 Zurich, Switzerland.

‡ Present address: Analytical and Nuclear Chemistry Division, Chemical and Material Sciences Directorate, Lawrence Livermore National Laboratory L-231, Livermore, CA 94550.

§ Deceased: July 30, 2001.

69%), encountered during the field experiments. This paper describes a potentially generalizable methodology for increasing the temporal and size resolution of atmospheric aerosol chemical composition measurements, using tandem ATOFMS-impactor sampling.

Introduction

Over the past decade, a number of research groups have developed mass spectrometry instruments that measure the size and chemical composition of individual particles in real-time (see Refs 1-3 for reviews). The development of these measurement techniques has been identified as the most significant advance in aerosol instrumentation during recent years (*4*). Although single-particle mass spectrometry instruments differ from one another in their particle sizing techniques, the vast majority obtain chemical composition information by laser ablation/ionization of individual particles and subsequent analysis of the ion mass spectra. A commonly cited limitation of single-particle mass spectrometry instruments is that the chemical composition measurements are not quantitative (*2*, *3*). There are two main obstacles to quantitation. First, the ion signal intensities produced by laser ablation/ionization of nominally identical particles vary greatly from shot-to-shot (*5*), primarily because of inhomogeneities in the ablation/ionization laser beam (*6*). Second, instrument sensitivities to different aerosol-phase chemical species are largely unknown. In the present work, *instrument sensitivity* is defined as the ion signal intensity per unit mass of a chemical species, averaged over a particle ensemble.

It has been reported that shot-to-shot variations in the ion signal intensities can be mitigated by using very high laser irradiances, but molecular information is lost due to fragmentation of polyatomic ions (*7*). For example, laser irradiances $>2 \times 10^{10}$ W cm^{-2} have been shown to fragment pure ammonium sulfate particles into monatomic N, H, S, and O (*7*). To retain molecular information, most single-particle mass spectrometry techniques use moderate laser irradiances ($\sim10^7$–10^9 W cm^{-2}). Operating at moderate irradiances, it is not yet possible to quantify the chemical composition of individual particles due to the shot-to-shot variations in ion signal intensities described above. However, it may be possible to quantify the chemical composition of small ensembles of single particles if the mass spectra from a collection of nominally identical particles are obtained and averaged (*5*, *8*).

Quantifying aerosol chemical composition from an ensemble of single-particle spectra requires a knowledge of instrument sensitivities to each chemical species in the particle ensemble. Instrument sensitivities can vary dramatically from one chemical species to another (*8*, *9*), due to chemically specific differences in ionization efficiency. To date, all efforts to determine instrument sensitivities have been based on particles generated in laboratory environments (*5*, *7–10*). These laboratory-generated particles are typically monodisperse, spherical, and have nominally identical chemical compositions. By comparing the average ion signal intensities obtained from 20 or more identical particles to the known chemical composition of the particle ensemble, investigators have been able to determine instrument sensitivities to a few chemical species under controlled laboratory conditions (*5*, *8*). Recent studies revealed that instrument sensitivities can be affected substantially by the size of the individual particle being sampled (*8*, *11*), trace

impurities in the particle matrix (*12*), and relative humidity of the background gas (*13*). Due to an incomplete understanding of these effects, extrapolation of the instrument sensitivities derived from simple laboratory-generated particles to the more complex atmospheric particles has not been successfully demonstrated.

In contrast to the laboratory-based approach described above, a *field-based approach* for determining instrument sensitivities would rely entirely on atmospheric particle measurements. Instrument sensitivities determined from a field-based approach would be directly applicable to ambient aerosol data. Moreover, a field-based approach can potentially elucidate the relative influences of particle size, particle composition, and meteorology, on instrument sensitivities under ambient sampling conditions. Ideally, the instrument sensitivities deduced from a field-based approach may be verified and further tested in laboratory experiments. Although a field-based approach for determining instrument sensitivity is appealing, it is subject to three limitations which are not encountered in a laboratory-based approach. First, a field-based approach requires quantitative reference measurements of the chemical species of interest to be taken in parallel with the single-particle measurements, because the chemical composition of an atmospheric aerosol is unknown at the time of sampling. Consequently, the accuracy of instrument sensitivities determined from a field-based approach is limited by the precision of the reference measurements. Second, a field-based approach requires the collection of a much larger number of single-particle spectra than are needed for most laboratory-based approaches, to obtain a statistically significant number of nominally identical particles from the complex mixture of particle types in the atmosphere. Third, particle detection efficiencies of the single-particle instrument must be well characterized to ensure the success of a field-based approach. Unlike the laboratory-generated particles, atmospheric aerosols are distributed by size, chemical composition, density, and morphology, all of which can influence the particle detection efficiency of a single-particle instrument (*14, 15*).

In the present study, we describe a field-based approach for determining single-particle instrument sensitivities that addresses the three limitations listed above. Our approach uses parallel measurements of atmospheric particles taken by an aerosol time-of-flight mass spectrometry (ATOFMS) instrument and a cascade impactor. ATOFMS is a rapidly developing and increasingly accepted single-particle mass spectrometry technique. ATOFMS instruments have been deployed in numerous field campaigns, yielding very large data sets ($\sim10^4$–10^6 spectra) of ambient single-particle size and chemical composition (*16*–*22*). Recently, Allen et al. developed a procedure for determining ATOFMS particle detection efficiencies under ambient sampling conditions (*14*). After the single-particle spectra are duplicated to correct for particle undercounting, ATOFMS ion signal intensities can be compared quantitatively with collocated cascade impactor measurements of aerosol chemical composition, yielding instrument sensitivity factors that can be used to quantify the chemical composition of size-segregated atmospheric particle ensembles.

The procedure is developed using ATOFMS and impactor measurements of ammonium and nitrate, taken at Riverside, CA, in September 1996, August 1997, and October 1997. ATOFMS instrument sensitivities, determined from the ATOFMS-impactor comparisons, are used to reconstruct continuous time series of quantitative, size-segregated NH_4^+ and NO_3^- measurements over the 0.32–1.8 μm aerodynamic diameter (D_a) range. The applicability of the instrument sensitivity factors derived in this paper to other aerosol data sets, collected at locations where different ATOFMS instrument designs are used and different particle types are

abundant, remains to be tested. However, application of the ATOFMS-impactor comparison methodology described herein to other atmospheric data sets will be straightforward. In the future, it may be possible to extend the field-based approach to single-particle mass spectrometry instruments other than ATOFMS and to aerosol species other than NH_4^+ and NO_3^-. The purposes of the present paper are to develop a field-based approach for determining ATOFMS instrument sensitivities and to illustrate some applications of the NH_4^+ and NO_3^- sensitivity factors.

Related Studies

Prior to this work, two quantitative comparisons of ATOFMS data with collocated measurements of atmospheric aerosol chemical composition have been reported in the literature. Liu et al. (*23*) compared the number of nitrate-containing particles detected by an ATOFMS instrument (defined as those particles which yielded an ion signal at mass-to-charge ratio 30 (NO^+) with relative intensity greater than 2%) with collocated NO_3^- mass concentration measurements taken by an automated nitrate monitor (*24*), at 10-minute sampling intervals. The numbers of nitrate-containing particles detected by ATOFMS exhibited a linear correlation ($R^2 = 0.73$) with the automated nitrate monitor measurements throughout the 53-h sampling event at Riverside, CA, demonstrating the ability of an ATOFMS instrument to track atmospheric NO_3^- concentrations based on the presence of a specific chemical marker (NO^+) in the single-particle mass spectra (*23*).

Fergenson et al. (*25*) applied a multivariate calibration technique to compare ATOFMS data with collocated impactor measurements of 44 different aerosol-phase chemical species taken at Riverside, CA, on September 23–26, 1996. In that study, ATOFMS data were grouped into a large number ($\sim$600–700) of clusters based on similar features of the single-particle mass spectra. The masses of each particle cluster were compared with collocated impactor measurements by the partial least-squares algorithm, yielding multivariate linear regression coefficients that relate the cluster masses with the atmospheric concentrations of 44 different aerosol-phase chemical species. Using 11 data cohorts as calibrants and one as a predictor, it was possible to evaluate the predictive value of the multivariate calibrations. The good overall agreement ($R^2 = 0.83$) between impactor measurements and the multivariate calibrated ATOFMS data presented in that study provides further evidence that ATOFMS data can potentially yield quantitative measurements of atmospheric aerosol chemical composition (*25*).

Both of the previous studies compared quantitative, bulk measurements of atmospheric aerosol chemical composition with the presence and abundance of specific *particle types* detected by ATOFMS. This paper differs from previous studies because it presents the first comparison of *ion signal intensities* measured by a single-particle mass spectrometry instrument with quantitative, bulk measurements of atmospheric aerosol chemical composition. A unique advantage of the present approach is that instrument sensitivities can be deduced from atmospheric aerosol data. In the future, these sensitivity factors can be verified and further tested under controlled laboratory conditions. As such, the results of the present paper can assist in the design of laboratory experiments aimed at quantifying the chemical composition of aerosols by single-particle mass spectrometry.

Experimental Method

The data presented in this paper were collected as part of four multisite field experiments that are described in detail elsewhere (*19, 26*–*30*). During each of these experiments, individual atmospheric particles were sampled continuously

TABLE 1. Intensive Operating Periods at Riverside, California

field experiment	IOP code	date	time	temp (°C)	RH (%)	number of spectra acquired by ATOFMS		
						0.32–0.56 μm	0.56–1.0 μm	1.0–1.8 μm
1996 Marine Particle Transport Study	T96-a	23 Sep 96	1500–1900 PDT	25.1	43.1	219	372	889
1996 Marine Particle Transport Study	T96-b	24 Sep 96	1500–1900 PDT	30.2	42.6	601	1462	1275
1996 Marine Particle Transport Study	T96-c	25 Sep 96	1500–1900 PDT	27.4	48.4	504	1547	1130
1996 Marine Particle Transport Study	T96-d	26 Sep 96	1500–1900 PDT	27.6	68.6	644	1643	843
SCOS97[a] First Vehicle Study	V1-a	21 Aug 97	1400–1800 PDT	34.2	27.6	472	679	650
SCOS97 First Vehicle Study	V1-b	22 Aug 97	1400–1800 PDT	35.0	27.5	574	675	571
SCOS97 Second Vehicle Study	V2-a	27 Aug 97	1400–1800 PDT	32.3	28.5	125	74	678
SCOS97 Second Vehicle Study	V2-b	28 Aug 97	0600–1000 PDT	22.9	57.1	311	273	747
SCOS97 Second Vehicle Study	V2-c	28 Aug 97	1355–1800 PDT	30.9	33.7	351	322	649
SCOS97 Third Nitrate Study	N3-a	31 Oct 97	0955–1353 PST	28.1	21.2	263	1009	1499
SCOS97 Third Nitrate Study	N3-b	31 Oct 97	1450–1810 PST	26.5	29.9	291	1253	1907

[a] 1997 Southern California Ozone Study.

by an ATOFMS instrument stationed at Riverside, CA. In addition, a collocated micro-orifice impactor collected size-segregated samples of the fine ambient aerosol ($D_a < 1.8$ μm) during selected time periods. The periods of tandem ATOFMS-impactor sampling are referred to hereafter as intensive operating periods (IOPs). Data from 11 IOPs are analyzed in this work (see Table 1).

Aerosol Measurements. Operating principles of the ATOFMS instrument stationed at Riverside during the IOPs are described in detail elsewhere (*16*, *31*, *32*), so only a brief overview is given here. Ambient particles are drawn into the ATOFMS instrument through a converging nozzle where they are accelerated to terminal velocities that are a function of their aerodynamic diameters. Next, each particle enters a sizing region where it passes through and scatters light from two continuous wave lasers separated by a known distance. The time difference between the scattering pulses indicates the velocity of the particle, which is recorded and later used to determine the particle aerodynamic diameter. The time difference between scattering pulses is also used to actuate the firing of a high power pulse from a Nd:YAG laser, operating at 266 nm wavelength and $2 \times 10^7 – 4 \times 10^8$ W cm^{-2} irradiance, upon the particle's arrival in the source region of a time-of-flight mass spectrometer. The ion signals resulting from ablation/ionization of a single particle by the Nd:YAG laser are detected by a dual microchannel plate and digitized using an 8-bit data acquisition board (Signatec, Model DA500), interfaced to a personal computer. The digitized mass spectrum is later analyzed to determine the chemical composition of the particle. Although field-transportable ATOFMS instruments are capable of dual ion acquisition (*33*), the ATOFMS instrument stationed at Riverside (*16*) was configured to analyze only positive ions during the IOPs. The number of positive ion mass spectra collected by ATOFMS during each IOP, as a function of D_a, are listed in Table 1.

A summary of impactor operations and sample analyses relevant to the present paper is presented here; detailed descriptions can be found elsewhere (*26*, *27*, *29*). Size-segregated particles were collected on Teflon impaction substrates loaded in a 10-stage micro-orifice impactor (MSP Corporation, Model 110) (*34*). Fine particles ($D_a < 1.8$ μm) in the Los Angeles atmosphere are generally sticky enough to avoid particle bounce problems within the impactor (*35*). Coarse particles ($D_a > 1.8$ μm), which are more likely to bounce off their intended impactor stage, were removed by Teflon-coated AHIL-design cyclone separators positioned upstream of the impactor inlets. No coatings were applied to the impaction substrates. After each IOP, the substrates were removed immediately and refrigerated until analysis,

to prevent volatilization losses. The size-segregated particle ensembles on each impaction substrate were analyzed by ion chromatography (Dionex Corp, Model 2020i) for NO_3^- (*36*) and by an indophenol colorimetric procedure for NH_4^+ (*37*) using an Alpkem rapid flow analyzer (Model RFA-300). Impactor measurements of NH_4^+ and NO_3^- in three aerodynamic diameter ranges, 0.32–0.56 μm, 0.56–1.0 μm, and 1.0–1.8 μm, are selected for the present analysis because particles collected on these three impactor stages span the overlapping aerodynamic size range of the ATOFMS instrument and the impactor. Data collected from the chemical analyses of 33 impaction substrates (11 IOPs $\times$ 3 D_a ranges) are used in this work.

The mass of NH_4^+ measured on three of the impaction substrates was found to be less than that measured on "blank" substrates which were unexposed to ambient aerosols, due to a combination of analytical error and low atmospheric NH_4^+ concentrations, yielding "negative" impactor measurements after blank subtraction. In ATOFMS measurements, ion signal intensities are non-negative by definition, and there is no data analysis procedure analogous to blank subtraction. To avoid introducing a positive bias in the ATOFMS-impactor comparisons, NH_4^+ measurements from the three affected impactor samples are excluded from the present analysis. These samples contained (1) 1.0–1.8 μm particles collected at 1400–1800 PDT on August 22, 1997, (2) 0.56–1.0 μm particles collected at 1400–1800 PDT on August 27, 1997, and (3) 1.0–1.8 μm particles collected at 1400–1800 PDT on August 27, 1997. In total, 30 impactor measurements of NH_4^+ and 33 impactor measurements of NO_3^- are compared with the corresponding ATOFMS data.

ATOFMS Data Treatment. Before ATOFMS and impactor measurements can be compared with each other, the measurements which best represent ATOFMS instrument responses to NH_4^+ and NO_3^- must be selected, and the ATOFMS data must be corrected for certain sampling biases.

ATOFMS Response Functions. To compare ATOFMS data with quantitative measurements of NH_4^+ and NO_3^-, a measure of the ATOFMS instrument's response to NH_4^+ and NO_3^- must be precisely defined. Ion signals indicating the presence of NH_4^+ in an individual particle are detected most often at mass-to-charge (*m/z*) ratio 18, when sampling Riverside aerosols by ATOFMS (*16*). The ion signal at *m/z* 30 (NO$^+$) is an established measure of aerosol nitrate at Riverside (*23*). Ion signals at other *m/z* ratios (e.g. *m/z* 35 (NH$_4$NH$_3^+$), *m/z* 46 (NO$_2^+$), and *m/z* 108 (Na$_2$NO$_3^+$)) also indicate the presence of NH_4^+ and NO_3^- in atmospheric particles (*23*). As a first approximation, only the ion signals at *m/z* 18 and 30 are considered because they are the most common and pro-

nounced indicators of NH_4^+ and NO_3^- in positive ion ATOFMS measurements of Riverside aerosols. The validity of this approximation is discussed later. In ATOFMS positive ion spectra, the presence of particulate H_2O is typically indicated by a peak at m/z 19 (H_3O^+) (16) and therefore does not augment the NH_4^+ signal at m/z 18.

Ion signals at m/z 18 and 30 are also detected when the ablation/ionization laser fragments certain nitrogen-containing organic compounds (38−40). However, NH_4NO_3 typically comprises the largest fraction of fine particle mass sampled at Riverside (26, 27, 30), so we expect the contributions of fragmented nitrogen-containing organic compounds to the ion signals at m/z 18 and 30 to be negligible relative to the contributions from NH_4^+ and NO_3^-. The validity of this assumption is discussed later.

Although there are several possible measures of ion signal intensity, absolute area and relative area are the most appropriate for quantification of mass spectrometry data. In laboratory ATOFMS studies of nominally identical particles, shot-to-shot variations caused the absolute areas of specific ion signals to vary by an average of 59%. During the same studies, relative areas, defined as the absolute area of the ion signal of interest divided by the total area of the mass spectrum, varied by an average of only 16% (9). This evidence suggests that relative areas should be used for quantification of ATOFMS data. However, when sampling a polydisperse multicomponent aerosol, such as that found in an urban atmosphere, relative area measurements can be affected greatly by the presence of additional chemical species in the particle. For example, the relative area of an ion signal at m/z 18 produced from ablation/ionization of a pure NH_4NO_3 particle will likely be larger than the relative area at m/z 18 measured from an identical particle that also contains a trace amount of potassium, because potassium is efficiently ionized (9) and will therefore increase the total area of the mass spectrum. Hence, relative area is not a stable measure of ion signal intensity when determining instrument sensitivities by a field-based approach. Instead, absolute area is selected as the measure of ion signal intensity in the present work. For the remainder of this paper, we define the ATOFMS instrument response to NH_4^+, $Resp_{NH_4^+}$, as the absolute area of the ion signal at m/z 18 $\pm$ 0.5 Daltons, and the ATOFMS response to NO_3^-, $Resp_{NO_3^-}$, as the absolute area of the ion signal at m/z 30 $\pm$ 0.5 Daltons.

During the IOPs, ion signals produced by ablation/ionization occasionally exceeded the dynamic range of the data acquisition board. In the present study, a slight (3.3%) measurement bias caused by dynamic range exceedances was observed and corrected accordingly, as described in the Supporting Information. In addition, 3.2% of the ATOFMS responses to NH_4^+ and 2.8% of the responses to NO_3^- exceeded the dynamic range of the data acquisition board. At these low levels, dynamic range limitations of the data acquisition board should not have a significant effect on the results of the present study.

Corrections for Particle Detection Efficiency. Allen et al. determined that ATOFMS instruments undercount particles by a factor, ϕ, that follows a power law dependence on aerodynamic particle diameter (14)

$$\phi = \alpha D_a^{\beta} \quad (1)$$

where parameters α and β are determined by nonlinear regression of impactor mass concentrations on the number of particles detected by ATOFMS, aggregated into 10 narrow size intervals fitting within each of the larger impactor size intervals (14). In the present work, the procedure of Allen et al. is modified slightly such that the nonlinear regression parameters, α and β, are determined from the ATOFMS

TABLE 2. Parameter Values and 95% Confidence Intervals Fit to the ATOFMS Particle Detection Efficiency Function $\Phi = \alpha D_a^{\beta}$

field experiment	α	β	no. of samples for comparison
1996 Marine Particle Transport Study[a]	5040 ± 1190	−3.13 ± 0.64	12
SCOS97[b] First Vehicle Study	1450 ± 434	−3.90 ± 0.52	6
SCOS97 Second Vehicle Study	2050 ± 624	−4.46 ± 0.46	9
SCOS97 Third Nitrate Study	5130 ± 2140	−4.68 ± 1.04	6

[a] In ref 14, α = 4999 ± 998 and β = −3.236 ± 0.520. [b] 1997 Southern California Ozone Study.

single-particle measurements of D_a, rather than assuming an average diameter for all particles within each narrow size interval. This subtle modification is described in the Supporting Information.

ATOFMS particle detection efficiencies varied gradually from one field experiment to the next, as a result of a routine instrument cleaning procedure that inadvertently modified the inlet nozzle dimensions. To account for the inlet modifications, best-fit values of the nonlinear regression parameters in eq 1 are calculated separately for each field study (see Table 2). Note that the first two field studies in 1997 (V1 and V2) were spaced 1 week apart from each other, whereas the second and third studies (V2 and N3) were conducted 3 months apart (see Table 1). During the interim periods, the instrument inlet was routinely cleaned. The larger change in parameter values between V2 and N3, relative to the modest change between V1 and V2 (see Table 2), reflects the cumulative effect of the inlet cleaning procedure on ATOFMS transmission efficiencies over the 3 month interim period. The slight differences between the 1996 parameter values shown in Table 2 and those reported previously (14), result from the regression model revision described above. Using the parameter values listed in Table 2, each single-particle mass spectrum obtained by ATOFMS is duplicated by a dimensionless factor, ϕ (see eq 1), which accounts for the degree to which particles of a given size were undercounted by ATOFMS during the given experiment. Allen et al. demonstrated that ATOFMS particle detection efficiencies during the 1996 Marine Particle Transport Study were not significantly affected by chemical composition, when averaged over the size-segregated ambient aerosol (14). By a similar analysis, no clear evidence could be found to indicate that chemical composition affected ATOFMS particle detection efficiencies during the 1997 field experiments. Therefore in the present work, ATOFMS data corrected for particle detection efficiencies are assumed to have the same chemical composition as the particle spectra from which they were duplicated.

ATOFMS−Impactor Data Comparison. Having corrected the ATOFMS measurements for detection biases, a quantitative comparison of the ATOFMS and impactor data can be made. The purpose of this comparison is to determine ATOFMS instrument sensitivities to NH_4^+ and NO_3^- in size-segregated atmospheric particles under the sampling conditions encountered during the IOPs at Riverside. Recall that instrument sensitivity is defined as the ion signal intensity per unit mass of a chemical species, averaged over a particle ensemble. In the present study, we compare large ensembles of single-particle ATOFMS data with collocated impactor measurements of NH_4^+ and NO_3^-. The ATOFMS spectra recorded during each IOP are segregated into three aerodynamic diameter intervals: 0.32−0.56 μm, 0.56−1.0 μm,

and $1.0-1.8\ \mu$m. This size-segregation yields 33 ensembles of ATOFMS spectra (11 IOPs $\times$ 3 D_a ranges) which can be compared with corresponding impactor measurements, using a regression model of the form

$$m_{ik} = \frac{\sum_{j \subset i} \phi_j \text{Resp}_{jk} \psi_{jk}}{V_i} + \epsilon_{ik} \tag{2}$$

In eq 2, the subscript i represents the particle ensemble within a specified aerodynamic diameter interval, sampled during a given IOP. The subscript j represents an ATOFMS single-particle measurement, and k represents the chemical species of interest. The mass concentration of species k (μg m^{-3}), from the impactor measurement of ensemble i, is designated as m_{ik}. The dimensionless factor ϕ_j is used to correct for the undercounting of particles by ATOFMS. For each particle j detected by ATOFMS, ϕ_j is calculated from the corresponding ATOFMS measurement of aerodynamic diameter, $D_{a,j}$, using eq 1. The ATOFMS instrument response (ion signal area units) to species k in particle spectrum j, defined earlier, is designated as Resp_{jk}. The variable ψ_{jk} represents the reciprocal of the ATOFMS instrument sensitivity (μg/ion signal area) to species k in particle j. The volume of air (m^3) sampled by ATOFMS, during the IOP when particle ensemble i was analyzed, is designated V_i. Calculation of V_i is described in the Supporting Information. The residual mass concentration (μg m^{-3}) of species k in ensemble i, unexplained by the regression model, is denoted as ϵ_{ik}. In the following section, we seek a physically meaningful parametrization of ψ_{jk} that minimizes the sum of squared residuals, $\sum_i \epsilon_{ik}^2$, in eq 2. All calculations are performed using the Matlab statistics package (The MathWorks, Natick, MA) and facilitated by the YAADA data analysis system (*41*).

Results

Figure 1 illustrates a first-order comparison of the ATOFMS and impactor measurements of NH$_4^+$ and NO$_3^-$. The vertical coordinates of each data point represent ATOFMS measurements, $\sum_{j \subset i} \phi_j \text{Resp}_{jk}/V_i$, after correcting for particle detection efficiencies. The horizontal coordinates of each data point represent the impactor measurement, m_{ik}, with horizontal error bars spanning ± 2 standard deviations, as determined from the repeated analysis of a fraction of the impactor samples and from consistency in the repeated analyses of a set of standards. It is important to emphasize that the vertical coordinates of each data point represent the ATOFMS measurements of a size-segregated ensemble of individual particles sampled during the indicated IOP. The number of single-particle measurements represented by each data point is listed in Table 1. Data points are plotted with different symbols and shading patterns, to represent data collected during different IOPs and in different particle size intervals, respectively.

Without any prior knowledge of the numerous factors that can affect ATOFMS instrument sensitivities, one might hypothesize that ion signal intensities are linearly correlated with the mass of a chemical species of interest (i.e. $\psi_{jk} =$ constant). If this were the case, all of the data points in Figure 1a,b would lie along a straight line ($R^2 = 1.0$). Instead, the data points appear to be clustered along separate lines as a function of particle size range, indicating that ψ_{jk} is strongly influenced by the size of the particle sampled. The ratio of a data point's vertical coordinate to its horizontal coordinate is generally largest for particle ensembles in the $0.32-0.56$ μm D_a range and smallest for ensembles in the $1.0-1.8$ μm range, for both NH$_4^+$ and NO$_3^-$ (see Figure 1). This suggests that the ion signal intensity produced by laser ablation/ionization of a unit mass of either species (NH$_4^+$ or NO$_3^-$) decreases as particle aerodynamic diameter increases over
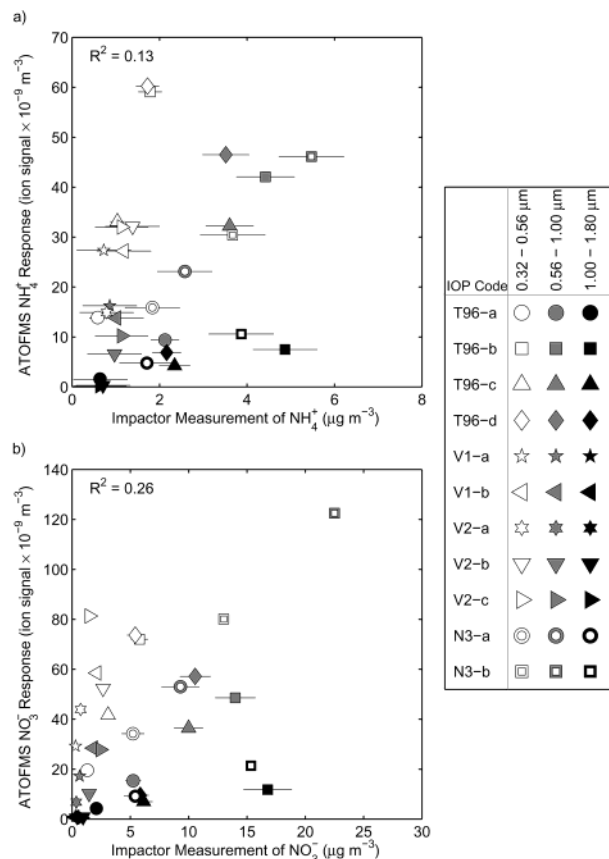
FIGURE 1. First-order comparison of impactor measurements with corresponding ATOFMS measurements, duplicated to correct for particle detection efficiencies. Horizontal error bars indicate ± 2 standard deviations in the impactor measurements. In cases where ± 2 SD is small relative to the horizontal axis scale, the error bars may be covered entirely by the plotting symbol and, therefore, not visible. IOP codes are defined in Table 1.

the $0.32-1.8$ μm range. In other words, ATOFMS instruments are more sensitive to NH$_4^+$ and NO$_3^-$ when sampling smaller particles. The increased instrument sensitivity to chemical species in smaller particles is presumed to be due to (1) a greater volume fraction of small particles being vaporized by the ablation/ionization laser relative to larger particles and (2) a lower probability of positive-negative charge recombination in the ablation plume of small particles relative to larger ones (*11*). Similar trends have been reported in single-particle mass spectrometry analyses of pure, laboratory-generated RbNO$_3$, (NH$_4$)$_2$SO$_4$, NaCl, and KCl particles (*8, 11, 42*), but this is the first such observation in atmospheric aerosol measurements.

Particle Size-Dependent Parametrization of Instrument Sensitivity. Further analyses of the trends in Figure 1 indicate that instrument sensitivity can be parametrized by a power law relationship in aerodynamic diameter

$$\psi_{jk} = \gamma_k D_{a,j}^{\delta_k} \tag{3}$$

where ψ_{jk} represents the inverse ATOFMS sensitivity (μg/ion signal area) to species k in particle j, $D_{a,j}$ is the single-particle aerodynamic diameter (μm) measured by ATOFMS, and γ_k and δ_k are nonlinear regression parameters, specific to chemical species k but independent of particle size, that can be determined using the regression model in eq 2. No major changes were made to the instrument's ablation/ionization configuration between the IOPs, so γ_k and δ_k are assumed to be constant across all four field experiments. Pooling data from all four experiments permits an evaluation of the stability

TABLE 3. Parameter Values and 95% Confidence Intervals Fit to the ATOFMS Instrument Sensitivity Function $\Psi = \gamma D_a^{\delta}$

species	γ	δ	no. of samples for comparison
NH_4^+	$2.5 \times 10^{-10} \pm 0.4 \times 10^{-10}$	2.4 ± 0.4	30
NO_3^-	$4.7 \times 10^{-10} \pm 0.7 \times 10^{-10}$	2.4 ± 0.4	33

of instrument sensitivities to NH_4^+ and NO_3^- during 11 IOPs spaced over a 1-year time period.

The power law form of eq 3 can be related to the physical and chemical factors that influence ATOFMS instrument sensitivities to NH_4^+ and NO_3^- under ambient sampling conditions. In eq 3, γ_k can be treated as a surrogate measure of the ionization efficiency of chemical species k. In general, chemical species which are efficiently ionized should have a smaller γ value than species which are more difficult to ionize. Therefore, best-fit values of $\gamma_{NH_4^+}$ and $\gamma_{NO_3^-}$ are expected to be different.

In eq 3, δ_k can be considered a surrogate measure of the volumetric fraction of an individual particle that is vaporized by the ablation/ionization laser, assuming that the increased probability of positive-negative charge recombination in the ablation plume of small particles has only a secondary effect. If $\delta_k \simeq 0$, instrument sensitivity is independent of particle size, implying that the ATOFMS ablation/ionization laser vaporizes either the entire particle volume or a constant volumetric fraction of each particle in the $0.32-1.8$ μm D_a range. If $\delta_k \simeq 3$, the instrument sensitivity is proportional to particle volume, implying that the laser vaporizes a constant volume of each particle in the $0.32-1.8$ μm range. A result of $0 < \delta_k < 3$ might suggest that small particles are completely vaporized, while particles at the upper end of the $0.32-1.8$ μm D_a range are only partially vaporized. Laboratory studies of ATOFMS instrument behavior indicate that laser irradiances similar to those used during the IOPs vaporize the entire volume of submicron particles but only partially vaporize particles that are larger than approximately 1.0 μm D_a (43). Hence, we expect best-fit values of $\delta_{NH_4^+}$ and $\delta_{NO_3^-}$ to fall in the intermediate range ($0 < \delta_k < 3$).

When a particle is partially vaporized by the ablation/ionization laser, the ATOFMS instrument is more likely to detect material near the particle surface than material in the particle core (44). NH_4^+ and NO_3^- are believed to have similar spatial distributions within the individual particle matrices studied here, because the origin of these two species in Riverside aerosols is largely attributed to the condensation of gas-phase ammonia and nitric acid molecules on the surface of pre-existing particles (45). Therefore in the present work, it is reasonable to assume that neither NH_4^+ nor NO_3^- will be preferentially vaporized in the event of partial vaporization. For this reason, the best-fit values of $\delta_{NH_4^+}$ and $\delta_{NO_3^-}$ deduced in the present work are expected to be similar.

Table 3 shows the best-fit values of γ_k and δ_k, along with 95% confidence intervals for each, as calculated by nonlinear regression using eqs 2 and 3. Note that the best-fit values of $\delta_{NH_4^+}$ and $\delta_{NO_3^-}$ are identical within two significant figures (2.4 ± 0.4), even though they were calculated independently using two different sets of measurements. Moreover, both δ values are in the $0-3$ range, as expected from the above discussion. These two observations support the physical explanation of the particle size-dependent instrument sensitivity parametrization (eq 3) and imply that NH_4^+ and NO_3^- do indeed have similar spatial distributions within the matrices of the larger particles studied here.

Best-fit values of $\gamma_{NH_4^+}$ and $\gamma_{NO_3^-}$ are statistically different from one another with 95% confidence (see Table 3), as we had expected from the discussion above. The ratio of these

two values can be used to determine the relative sensitivity of ATOFMS instruments to NH_4^+ versus NO_3^- as follows

$$\text{RSF}\left(\frac{NH_4^+}{NO_3^-}\right) = \frac{18}{62} \cdot \frac{\gamma_{NH_4^+}}{\gamma_{NO_3^-}} \qquad (4)$$

where 18 and 62 are the molar masses of NH_4^+ and NO_3^-, respectively. Relative sensitivity factors (RSFs) are typically defined on a molar basis and are often used to correct for differences between the instrument sensitivities to two chemical species of interest, when analyzing the composition of a multicomponent sample (9, 46). Prior to this study, all ATOFMS RSFs have been deduced from laboratory-generated aerosols (9, 39), and their applicability to ambient aerosol data has not been tested. Using eq 4 and the best-fit γ_k values listed in Table 3, the RSF of NH_4^+ versus NO_3^- under the Riverside IOP sampling conditions is 0.5 and lies in the $0.4-0.7$ range with 95% confidence. This implies that ATOFMS measurements of particles containing equimolar concentrations of NH_4^+ and NO_3^- should yield larger ion signals at m/z 30 than at m/z 18, by a factor of approximately two. The RSF derived above will be verified in laboratory experiments so that ultimately it may be used to determine the relative abundances of NH_4^+ and NO_3^- in individual atmospheric particles.

Scaled ATOFMS Measurements of NH_4^+ and NO_3^-. Using raw ATOFMS data and the best-fit parameter values listed in Tables 2 and 3, we can reconstruct quantitative measurements of NH_4^+ and NO_3^- mass concentrations, $\hat{m}_{ik}$, in size-segregated atmospheric particle ensembles.

$$\hat{m}_{ik} = \frac{\sum_{j \subset i} \phi_j \, \text{Resp}_{jk} \, \psi_{jk}}{V_i} \qquad (5)$$

All terms in eq 5 are defined in eqs 2 and 3. Scaled ATOFMS measurements are compared with the corresponding impactor measurements of atmospheric NH_4^+ and NO_3^- concentrations in Figure 2. The horizontal coordinate of each data point in Figure 2 represents an impactor measurement, m_{ik}, with error bars spanning ± 2 standard deviations. The vertical coordinate of each data point represents a scaled ATOFMS measurement, $\hat{m}_{ik}$, with error bounds calculated by propagating 95% confidence intervals on the best-fit values of γ_k and δ_k (see Table 3). Vertical error bars do not account for uncertainties in the ATOFMS particle detection efficiency parameters, α and β, but those uncertainties are discussed below in detail.

When evaluating the accuracy of the ATOFMS instrument sensitivity parametrization (eq 3), impactor data are used as the reference because impactors currently provide the most reliable data on size-segregated aerosol composition. However, impactor measurements of NH_4^+ and NO_3^- are subject to certain biases. Volatilization of NH_4NO_3 from impaction substrates during sampling is favored at high temperatures and low relative humidities (47) and has been shown to result in $7-8\%$ losses of fine particulate nitrate under hot (35 °C) and dry (18% relative humidity) conditions (35). Volatilization losses can be even greater ($\sim 10-20\%$) when aerosol loadings are low, because the exposed surface area of particle deposits is large relative to the aerosol mass collected on the impaction substrates (48). The possible effects of NH_4NO_3 volatilization on results of the present study are discussed later in this paper. Future applications of the tandem ATOFMS-impactor sampling procedure to less volatile chemical species (e.g. SO_4^{2-}) may permit a more accurate determination of ATOFMS instrument sensitivities.

One simple set of criteria for judging whether the ATOFMS scaling functions yield accurate measurements of atmo-
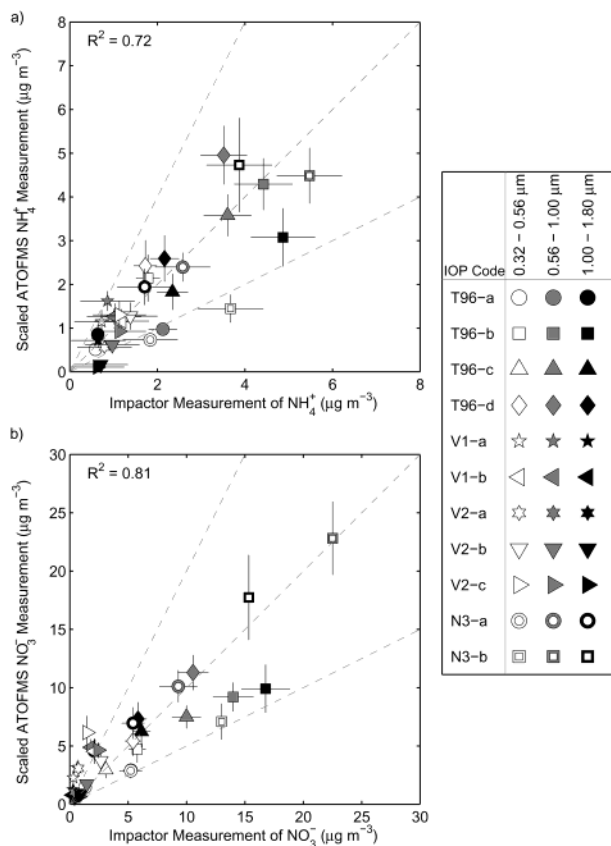
FIGURE 2. Comparison of scaled ATOFMS measurements with the corresponding impactor measurements. Diagonal dashed lines represent the 1:2, 1:1, and 2:1 lines of correspondence. Vertical error bars indicate 95% confidence intervals of the scaled ATOFMS measurements. Horizontal error bars indicate ± 2 standard deviations in the impactor measurements. In cases where an error bar length is small relative to the scale of the coordinate axes, it may be covered entirely by the plotting symbol and, therefore, not visible. IOP codes are defined in Table 1.

spheric NH_4^+ and NO_3^- concentrations is as follows. If a scaled ATOFMS measurement falls within ± 2 standard deviations of the corresponding impactor measurement, it is judged to be "excellent". If the 95% confidence interval of an ATOFMS measurement overlaps within ± 2 standard deviations of the corresponding impactor measurement, the ATOFMS measurement is considered to be "good". If neither of the above conditions are met, but the scaled ATOFMS measurement falls within a factor of 2 of the impactor measurement, it is judged as "fair". If none of these conditions are met, the ATOFMS measurement is "poor". The advantages of these evaluation criteria are that they account for the analytical error inherent in the impactor data, and the scaled ATOFMS measurements can be evaluated easily by visual inspection of Figure 2.

Using these criteria, 16 of the 30 scaled ATOFMS NH_4^+ measurements are excellent, 9 are good, 2 are fair, and only 3 are poor (see Figure 2a). The large fraction (90%) of "excellent", "good", and "fair" ATOFMS measurements indicate that the particle size-dependent parametrization of instrument sensitivity to NH_4^+ is stable over the range of fine particle concentrations encountered at Riverside ($PM_{1.8} = 17.58 \pm 2.02-127.8 \pm 1.76 \ \mu g \ m^{-3}$). All three of the "poor" ATOFMS NH_4^+ measurements are smaller than the corresponding impactor measurements, and one of these is largely due to inaccuracies in the ATOFMS particle detection efficiency, as discussed below. Of the 33 scaled ATOFMS NO_3^- measurements, 10 are excellent, 6 are good, 7 are fair,

and 10 are poor (see Figure 2b). All 10 of the "poor" ATOFMS NO_3^- measurements are greater than the corresponding impactor measurement, and, in all 10 cases, the impactor NO_3^- measurements are less than 2.1 $\mu g \ m^{-3}$ (see lower-left corner of Figure 2b). Moreover, 9 of the 10 poor measurements correspond to data collected during IOPs when the highest ambient temperatures were encountered (T > 30°C), suggesting that the impactor measurements during these periods may have been subject to volatilization losses. This issue will be explored later in the paper. The "excellent," "good", and "fair" NO_3^- measurements further increase our confidence in the selected parametrization of ATOFMS instrument sensitivity (eq 3). Recall that the data plotted in Figure 2 were collected during four field experiments spaced over a year, and the ATOFMS instrument's inlet design was modified between experiments. The lack of observable biases in the scaled ATOFMS measurements, obtained from data collected during different field experiments (compare positions of the experiment-specific plotting symbols relative to the 1:1 line), suggests that the instrument sensitivities to NH_4^+ and NO_3^- are unaffected by modifications to the instrument's inlet design.

A second set of criteria for evaluating the ATOFMS scaling functions employs statistical correlations of the impactor measurements with corresponding scaled ATOFMS measurements, irrespective of the error bounds on each. The advantage of using statistical correlations is that they may be used to estimate the relative influence of different parameters on ATOFMS instrument sensitivities. For example, scaled ATOFMS NH_4^+ measurements and corresponding impactor measurements exhibit a squared correlation coefficient (R^2) of 0.72. This indicates that approximately 72% of the variance in ψ_{j,NH_4^+} is explained by the size-dependent instrument sensitivity parametrization shown in eq 3. By an analogous calculation, 81% of the variance in ψ_{j,NO_3^-} is explained by the size-dependent sensitivity parametrization. These high correlation coefficients indicate that the most influential factor governing ATOFMS instrument sensitivities to NH_4^+ and NO_3^- is particle aerodynamic diameter, under the sampling conditions encountered at Riverside. Note that the R^2 values of 0.72 and 0.81 are significantly higher than those calculated under the assumption that instrument sensitivity is independent of particle size ($R^2 = 0.13$ in Figure 1a and $R^2 = 0.26$ in Figure 1b).

Attaining perfect correlations ($R^2 = 1.00$) is infeasible due to analytical error inherent in the impactor measurements, but it may be possible to reduce the sum of squared residuals further (i.e. increase R^2) by identifying measurable factors other than particle size which significantly influence ATOFMS instrument sensitivities. In the following section, we assess the relative influence of other factors on ATOFMS instrument sensitivities to NH_4^+ and NO_3^-, under the Riverside ambient sampling conditions.

Residual Analysis. Aside from particle size, the measurable factors which might also affect instrument sensitivities include (1) accuracy of the ATOFMS particle detection efficiency corrections; (2) properties of the background gas; (3) size-segregated aerosol chemical composition, as determined from chemical analyses of the impactor samples; and (4) single-particle chemical composition, as determined from ATOFMS ion signals measured at m/z ratios other than 18 and 30. To identify which of these factors significantly influenced ATOFMS sensitivities to NH_4^+ and NO_3^- during the IOPs, we examine the R^2 values of each factor with the residual concentrations, denoted as ϵ_{ik} in eq 2. For brevity, we discuss only those factors which show "strong evidence" of an influence on ATOFMS instrument sensitivities. Strong evidence is defined in the Supporting Information.

Influence of Particle Detection Efficiency Corrections. As stated earlier, one of the three main limitations of a field-based approach is that it requires an accurate characterization of the ATOFMS instrument's particle detection efficiency. In other words, each single-particle spectrum j must be duplicated by a precise particle detection efficiency factor, ϕ_j, to reconstruct accurate NH_4^+ and NO_3^- measurements from raw ATOFMS data (see eq 5). For a variety of reasons, it is not yet possible to determine precise values of ϕ_j under ambient sampling conditions (*14, 15*). Instead, particle detection efficiencies are approximated as a function of D_a (see eq 1), and these approximations are somewhat uncertain.

To assess the influence of particle detection efficiency uncertainties on the scaled NH_4^+ and NO_3^- measurements, we define a residual aerosol mass concentration ($\mu g\ m^{-3}$), ϵ_i, as

$$\epsilon_i = m_i - \sum_{j \subset i} \frac{\phi_j}{V_i} \rho_p \frac{\pi}{6} D_{p,j}{}^3 \tag{6}$$

where m_i is the mass concentration ($\mu g\ m^{-3}$) of particle ensemble i determined from gravimetric analysis of the impactor samples, and $\rho_p (\pi/6) D_{p,j}{}^3$ is the estimated mass of an individual particle detected by ATOFMS, assuming particles are spherical with density, $\rho_p = 1.3\ g\ cm^{-3}$, and physical diameter, D_p. Note that m_i and ϵ_i refer to total aerosol mass concentrations, whereas m_{ik} and ϵ_{ik} are specific to a chemical component (compare eqs 2 and 6). In short, $\epsilon_i < 0$ indicates that the particle detection efficiency correction factors applied to ATOFMS data collected from ensemble i are too large on average, whereas $\epsilon_i > 0$ indicates the correction factors are too small.

In cases where the particle detection efficiency correction factors applied to ATOFMS data are too large (i.e. $\epsilon_i < 0$), one would expect the scaled ATOFMS measurements of NH_4^+ and NO_3^- concentrations to exceed the corresponding impactor measurements ($\hat{m}_{ik} > m_{ik}$), and vice versa. This hypothesis is confirmed by examining the correlation of NH_4^+ and NO_3^- residuals with aerosol mass concentration residuals, illustrated in Figure 3. Both subplots show statistically significant positive correlations ($R^2 = 0.35$ for NH_4^+ and $R^2 = 0.36$ for NO_3^-), indicating that approximately 35% of the variance in ϵ_{ik} can be explained by a linear relationship with ϵ_i. In other words, approximately one-third of the error in the instrument sensitivities to NH_4^+ and NO_3^- is attributable to uncertainty in the ATOFMS particle detection efficiencies. This demonstrates a need to precisely characterize ATOFMS particle detection efficiencies, perhaps by comparing ATOFMS data with collocated particle number concentration data, which can be obtained continuously at very fine particle size and temporal resolutions.

Influence of Gas-Phase Properties. Neubauer et al. reported that relative humidity of the background gas can exert a strong influence on single-particle mass spectra (*13*), motivating the present analysis. Although our data set provided no clear evidence that instrument sensitivities to NH_4^+ nor NO_3^- are affected by ambient relative humidity over the 21–69% range, statistically significant negative correlations of ϵ_{ik} with ambient temperature ($R^2 = 0.14$ for NH_4^+ and $R^2 = 0.39$ for NO_3^-) indicate that scaled ATOFMS measurements of NH_4^+ and NO_3^- tend to exceed the corresponding impactor measurements when sampling at high temperatures. The highest ambient temperatures were encountered during the afternoon IOPs of August 1997 (V1-a, V1-b, V2-a, V2-c). This apparent temperature effect is most likely due to the condensation of gas-phase NH_3 and HNO_3 upstream of the ATOFMS instrument, which was stationed in an air condi-
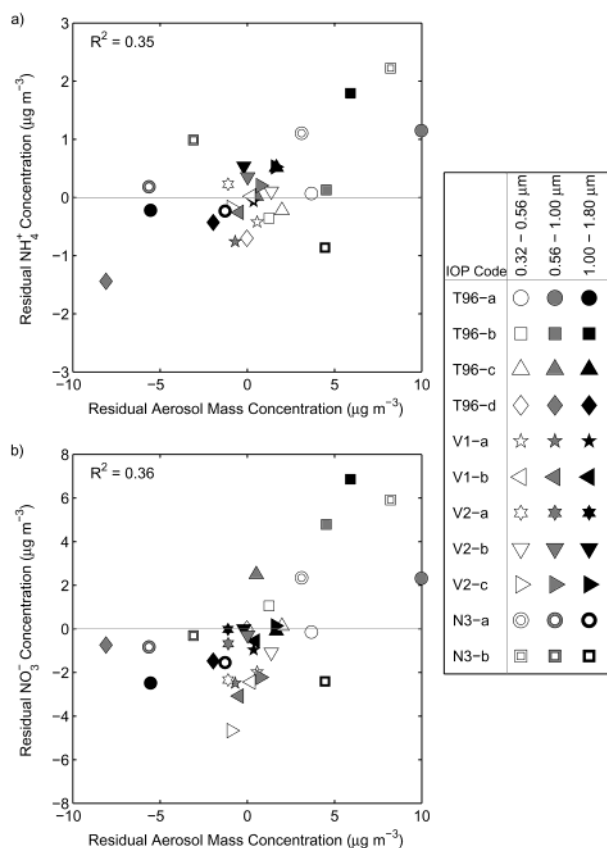

FIGURE 3. Comparison of residual species concentrations, ϵ_{ik}, with residual mass concentrations, ϵ_i. IOP codes are defined in Table 1.

tioned laboratory (T $\simeq$ 22–25 °C) and drawing ambient air through a ~5 m long sampling line at a relatively low flowrate. When the warmest temperatures were encountered (T $\geq$ 30.5 °C), high ambient concentrations of gas-phase NH_3 (23.8 $\pm$ 1.6–45.4 $\pm$ 1.5 $\mu g\ m^{-3}$) and HNO_3 (5.6 $\pm$ 0.6–9.3 $\pm$ 0.6 $\mu g\ m^{-3}$) were present (*27*). The apparent ATOFMS overestimates during the high-temperature IOPs, which include 90% of the "poor" ATOFMS NO_3^- measurements, might be entirely explained by NH_4NO_3 and HNO_3 condensation in the ATOFMS sampling line. In addition, volatilization of NH_4NO_3 from the impaction substrates during sampling may have decreased the impactor measurements of NH_4^+ and NO_3^- during the high-temperature IOPs by 10–20%, as discussed above.

Residual correlations indicate that the high-temperature sampling artifacts contribute 39% of the variance in ϵ_{i,NO_3^-}. To assess the effect of high-temperature sampling artifacts on the results of the present study, sensitivity parameters can be recalculated using the 21 data points corresponding to low-temperature IOPs (T < 30.5 °C). This recalculation does not affect the $\gamma_{NO_3^-}$ value shown in Table 3, but the best-fit $\delta_{NO_3^-}$ value is reduced from 2.4 $\pm$ 0.4 to 2.2 $\pm$ 0.4. In contrast with NO_3^-, only 14% of the variance in ϵ_{i,NH_4^+} can be explained by the high-temperature sampling artifacts. The effect on ATOFMS NH_4^+ measurements is less pronounced than on NO_3^- measurements because NH_3 has a higher vapor pressure than HNO_3, making it less likely to condense in the sampling line, and because three of the NH_4^+ measurements taken during high-temperature IOPs were excluded from the entire analysis, for reasons given above. Recalculation of the NH_4^+ regression coefficients using only the 21 low-temperature data points does not change the best-fit values of $\gamma_{NH_4^+}$ and $\delta_{NH_4^+}$ listed in Table 3. This suggests that the instrument

sensitivity parametrization (eq 3) for NH_4^+ is stable over the 23–35 °C temperature range. Average temperatures and relative humidities during each IOP are listed in Table 1.

Influence of Bulk Aerosol Composition. Laboratory studies of single-particle mass spectrometry instruments reveal that the presence of certain chemical species in a particle can dramatically affect the instrument response to other species present in the same particle (*12*). These phenomena, commonly referred to as *matrix effects*, have not yet been assessed under ambient sampling conditions. Extensive bulk aerosol composition data are available from chemical analyses of the impactor samples (*19, 26, 27, 30*), allowing us to assess whether chemical composition significantly affects ATOFMS instrument sensitivities to NH_4^+ and NO_3^-, when averaged over the size-segregated ambient aerosols studied here. Correlation coefficients of ϵ_{i,NH_4^+} and ϵ_{i,NO_3^-} with all analyte measurements that are greater than two standard errors above zero on at least half of the impaction substrates (mass, organic carbon, NH_4^+, NO_3^-, SO_4^{2-}, Na^+, La, and Sb) were calculated. No evidence of bulk compositional effects on ATOFMS instrument sensitivity to NH_4^+ was found. However, impactor measurements of aerosol mass, organic carbon, NH_4^+, NO_3^-, and SO_4^{2-}, all exhibit statistically significant negative correlations with ϵ_{i,NO_3^-} ($R^2 = 0.26-0.34$). These correlations are largely due to the ATOFMS-impactor measurement discrepancies during high-temperature IOPs. Without the high-temperature data points, none of the impactor measurements are correlated with ϵ_{i,NO_3^-}.

Based on these calculations, we conclude that aerosol chemical composition had an insignificant influence on the sensitivity of ATOFMS instruments to NH_4^+ and NO_3^-, when averaged over the size-segregated particle ensembles sampled at Riverside. It is important to note that NH_4^+ and NO_3^- comprise a large fraction of the aerosols studied in this work, so the ATOFMS instrument response to NH_4^+ and NO_3^- may be less influenced by matrix effects than the instrument response to other species. In addition, the aerosol mixtures during different IOPs may have been too similar to one another to reveal bulk compositional biases in the instrument sensitivities. In the future, it may be possible to elucidate such biases by comparing ATOFMS-impactor data sets collected at two geographic locations with very different aerosol compositions or by analyzing an ATOFMS-impactor data set collected at a single location over an extended study period that spans a significant change in bulk aerosol composition.

Influence of Single-Particle Composition. In eq 2, $Resp_{j,NH_4^+}$ and $Resp_{j,NO_3^-}$ are defined as the ion signals at m/z 18 and 30, respectively. To examine the influence of other ion signals on the scaled ATOFMS NH_4^+ and NO_3^- measurements, the correlations of ϵ_{i,NH_4^+} and ϵ_{i,NO_3^-} with all ion signal intensities in the $0 < m/z < 250$ Dalton range that appear in at least one particle spectrum in each size-segregated sample are calculated. In this analysis, ion signals are duplicated to account for ATOFMS particle detection efficiencies, and ion signals in the $0 < m/z < 60$ Dalton range are discarded from single-particle spectra in which an elevated noise level was observed, for reasons described in the Supporting Information.

Ion signals at 27 different m/z ratios exhibit statistically significant negative correlations with ϵ_{i,NH_4^+} ($0.14 \leq R^2 \leq 0.23$), indicating that NH_4^+ concentrations are overestimated when ion signals at these m/z ratios are abundant. Negative correlations may imply that (1) some fraction of the ion signals at m/z 18 resulted from aerosol species other than NH_4^+ and (2) the presence of other species in the aerosols increased the ionization efficiency of NH_4^+ (i.e. a matrix effect). Determining the most probable explanation for all 27 observed correlations is beyond the scope of this paper.

Moreover, many of these correlations are likely to be interrelated.

In laboratory-based ATOFMS studies, Angelino et al. discovered that ion signals at m/z 18 are commonly detected when sampling individual particles that contain organic amines (*40*). In ATOFMS data, the most common indicators of organic amines appear at m/z 58 and 86 (*40*). Ion signals at m/z 58 and 86 are among the 27 m/z ratios which are significantly correlated with residual NH_4^+ concentrations ($R^2 = 0.19$ and 0.16, respectively). Laboratory experiments are necessary to quantify and subtract the relative contribution of organic amine fragmentation from the total ion signal at m/z 18. If this approach proves to be feasible, it may be possible in the future to determine causes of the observed correlations with other ion signals.

Ion signals at each m/z ratio are uncorrelated with ϵ_{i,NO_3^-}, indicating that ions at m/z ratios other than 30 do not significantly influence scaled ATOFMS NO_3^- measurements in the Riverside aerosols. When sampling larger particle sizes ($D_a > 1.8$ μm) and/or marine aerosols, a significant fraction of the aerosol nitrate may be present in the form of $NaNO_3$. In these cases, it may be necessary to incorporate the ion signal at m/z 108 ($Na_2NO_3^+$) into the definition of $Resp_{NO_3^-}$.

Summary of Residual Analysis. The analyses described above indicate the relative influences of various measurable factors on ATOFMS instrument sensitivities to NH_4^+ and NO_3^-, under the Riverside sampling conditions. Aside from particle aerodynamic diameter, few factors significantly influenced the instrument sensitivities to NH_4^+ and NO_3^-. The second most pronounced influence is attributed to uncertainties in the ATOFMS particle detection efficiency. Sampling artifacts at high ambient temperatures contributed a significant fraction of the variance in ϵ_{i,NO_3^-}. Finally, a small fraction of the variance in ϵ_{i,NH_4^+} may be attributed to interfering ion signals at m/z 18 resulting from the fragmentation of organic amines, and to matrix effects that enhance the ionization of NH_4^+.

Discussion

The instrument sensitivity factors derived from tandem ATOFMS-impactor sampling can be used to reconstruct continuous ATOFMS measurements of size-segregated NH_4^+ and NO_3^- concentrations throughout the 1996 and 1997 field experiments, with very fine size resolution. For example, Figure 4a shows NH_4^+ measurements at Riverside, binned into 15 particle size intervals spanning the $0.32-1.80$ μm D_a range, and 24 4-h time intervals spanning 4 days of the 1996 Marine Particle Transport Study. Each row in Figure 4a can be translated into a conventional plot of NH_4^+ concentration as a function of particle size, during the specified 4-h sampling period. To illustrate this, Figure 4b,c shows size-resolved ATOFMS measurements of NH_4^+ concentration corresponding to the two highlighted rows of Figure 4a. Also, impactor measurements taken during the same time periods are plotted in Figure 4b,c, for the purpose of comparison. Similarly, Figure 5 illustrates the tandem ATOFMS-impactor NO_3^- measurements. High-resolution chemical composition measurements capture many of the detailed characteristics of the Riverside aerosol, which cannot be detected using impactors alone. For example, measurements taken during the September 25, 1996 IOP show sharp peaks at ca. 0.7 μm in the NH_4^+ and NO_3^- size distributions (see Figures 4c and 5c). Continuous measurements of size-resolved NH_4^+ and NO_3^- will substantially augment the amount of experimental data currently available for air quality model evaluations.

The applicability of the instrument sensitivity factors derived in this paper to other data sets, collected at locations where different ATOFMS instrument designs are used and
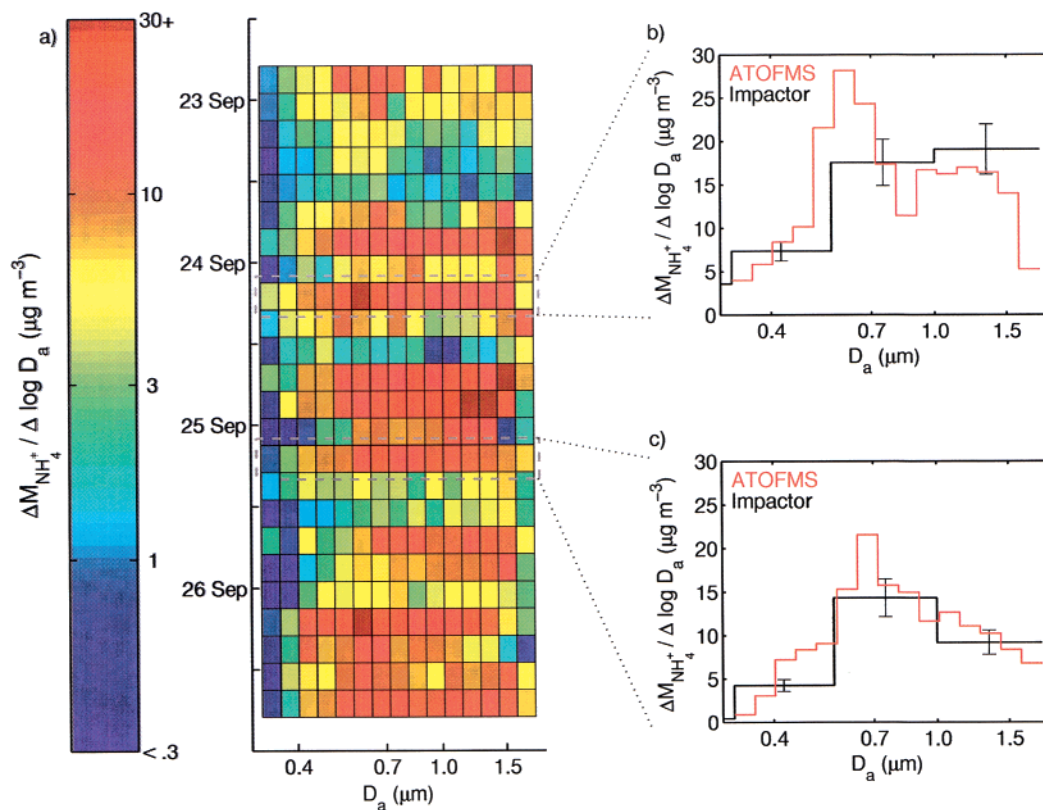
FIGURE 4. Ammonium mass distributions at Riverside. (a) Time series based on scaled ATOFMS measurements for 4-h intervals from September 23 through 27, 1996, with divisions at 0300, 0700, 1100, 1500, 1900, and 2300 PDT. (b) Scaled ATOFMS data and impactor data at 1500−1900 PDT on September 24, 1996. (c) Scaled ATOFMS data and impactor data at 1500−1900 PDT on September 25, 1996.
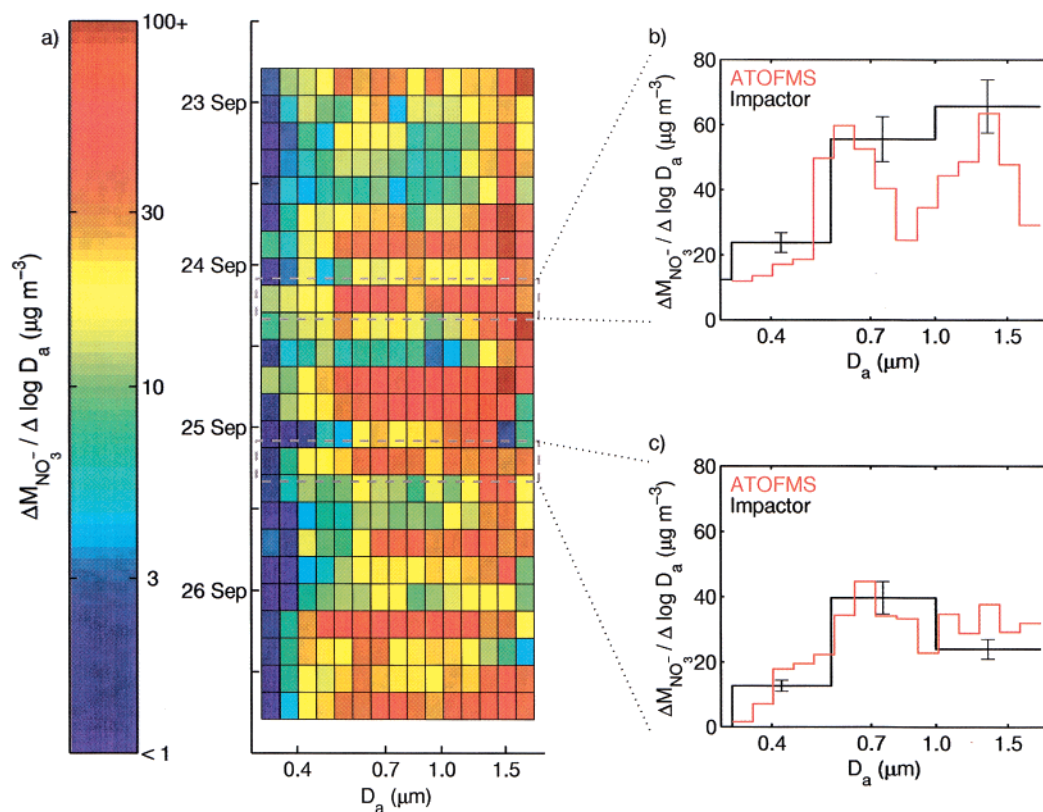

FIGURE 5. Nitrate mass distributions at Riverside. (a) Time series based on scaled ATOFMS measurements for 4-h intervals from September 23 through 27, 1996, with divisions at 0300, 0700, 1100, 1500, 1900, and 2300 PDT. (b) Scaled ATOFMS data and impactor data at 1500−1900 PDT on September 24, 1996. (c) Scaled ATOFMS data and impactor data at 1500−1900 PDT on September 25, 1996.

different particle types are abundant, remains to be tested. However, application of the methodology described herein to other tandem ATOFMS-impactor data sets will be straightforward. In future field experiments, collocated reference measurements of aerodynamic particle size distributions may yield more accurate determinations of the ATOFMS particle detection efficiencies, which in turn will improve the precision of the instrument sensitivity factors calculated using the field-based approach. In addition, laboratory experiments can be designed to test and verify the instrument sensitivities calculated in the present work. In the future, it may be possible to extend the field-based approach to single-particle mass spectrometry instruments other than ATOFMS and to aerosol species other than NH_4^+ and NO_3^-. Such applications remain to be tested. The strong influence of particle size on instrument sensitivities is an important conclusion of the present work. This size-dependence demonstrates a necessity for accurate particle sizing by single-particle instruments (49), if the field-based approach is to be successfully applied and further developed. In addition, collocated reference instruments must provide size-resolved aerosol chemical composition data, if they are to be used for the purpose of determining instrument sensitivities.

Acknowledgments

Supporting Information Available

Effects of exceeding the data acquisition board dynamic range, revised procedure for determining ATOFMS particle detection efficiencies, and criteria for evaluating the statistical significance of an R^2 value. This material is available free of charge via the Internet at http://pubs.acs.org.

Literature Cited

(1) Suess, D. T.; Prather, K. A. *Chem. Rev.* **1999**, *99*, 3007−3035.
(2) Noble, C. A.; Prather, K. A. *Mass Spectrom. Rev.* **2000**, *19*, 248−274.
(3) Johnston, M. V. *J. Mass Spectrom.* **2000**, *35*, 585−595.
(4) McMurry, P. H. *Atmos. Environ.* **2000**, *34*, 1959−1999.
(5) Mansoori, B. A.; Johnston, M. V.; Wexler, A. S. *Anal. Chem.* **1994**, *66*, 3681−3687.
(6) Rose, H. A.; DuBois, D. F. *Physics Fluids B* **1993**, *5*, 590−596.
(7) Reents, W. D.; Schabel, M. J. *Anal. Chem.* **2001**, *73*, 5403−5414.
(8) Ge, Z.; Wexler, A. S.; Johnston, M. V. *Environ. Sci. Technol.* **1998**, *32*, 3218−3223.
(9) Gross, D. S.; Gälli, M. E.; Silva, P. J.; Prather, K. A. *Anal. Chem.* **2000**, *72*, 416−422.
(10) Woods, E.; Smith, G. D.; Dessiatrik, Y.; Baer, T.; Miller, R. E. *Anal. Chem.* **2001**, *73*, 2317−2322.
(11) Carson, P. G.; Johnston, M. V.; Wexler, A. S. *Rapid Commun. Mass Spectrom.* **1997**, *11*, 993−996.
(12) Reilly, P. T. A.; Lazar, A. C.; Gieray, R. A.; Whitten, W. B.; Ramsey, J. M. *Aerosol Sci. Technol.* **2000**, *33*, 135−152.
(13) Neubauer, K. R.; Johnston, M. V.; Wexler, A. S. *Atmos. Environ.* **1998**, *32*, 2521−2529.
(14) Allen, J. O.; Fergenson, D. P.; Gard, E. E.; Hughes, L. S.; Morrical, B. D.; Kleeman, M. J.; Gross, D. S.; Gälli, M. E.; Prather, K. A.; Cass, G. R. *Environ. Sci. Technol.* **2000**, *34*, 211−217.
(15) Kane, D. B.; Johnston, M. V. *Environ. Sci. Technol.* **2000**, *34*, 4887−4893.
(16) Noble, C. A.; Prather, K. A. *Environ. Sci. Technol.* **1996**, *30*, 2667−2680.
(17) Liu, D.-Y.; Rutherford, D.; Kinsey, M.; Prather, K. A. *Anal. Chem.* **1997**, *69*, 1808−1814.
(18) Gard, E. E.; Kleeman, M. J.; Gross, D. S.; Hughes, L. S.; Allen, J. O.; Morrical, B. D.; Fergenson, D. P.; Dienes, T.; Gälli, M. E.; Johnson, R. J.; Cass, G. R.; Prather, K. A. *Science* **1998**, *279*, 1184−1187.
(19) Hughes, L. S.; Allen, J. O.; Bhave, P.; Kleeman, M. J.; Cass, G. R.; Liu, D.-Y.; Fergenson, D. P.; Morrical, B. D.; Prather, K. A. *Environ. Sci. Technol.* **2000**, *34*, 3058−3068.
(20) Guazzotti, S. A.; Whiteaker, J. R.; Suess, D.; Coffee, K. R.; Prather, K. A. *Atmos. Environ.* **2001**, *35*, 3229−3240.
(21) Guazzotti, S. A.; Coffee, K. R.; Prather, K. A. *J. Geophys. Res.* **2001**, *106*, 28607−28627.
(22) Whiteaker, J. R.; Suess, D.; Prather, K. A. *Environ. Sci. Technol.* **2002**, *36*, 2345−2353.
(23) Liu, D.-Y.; Prather, K. A.; Hering, S. V. *Aerosol Sci. Technol.* **2000**, *33*, 71−86.
(24) Stolzenburg, M. R.; Hering, S. V. *Environ. Sci. Technol.* **2000**, *34*, 907−914.
(25) Fergenson, D. P.; Song, X.-H.; Ramadan, Z.; Allen, J. O.; Hughes, L. S.; Cass, G. R.; Hopke, P. K.; Prather, K. A. *Anal. Chem.* **2001**, *73*, 3535−3541.
(26) Hughes, L. S.; Allen, J. O.; Kleeman, M. J.; Johnson, R. J.; Cass, G. R.; Gross, D. S.; Gard, E. E.; Gälli, M. E.; Morrical, B. D.; Fergenson, D. P.; Dienes, T.; Noble, C. A.; Liu, D.-Y.; Silva, P. J.; Prather, K. A. *Environ. Sci. Technol.* **1999**, *33*, 3506−3515.
(27) Allen, J. O.; Hughes, L. S.; Salmon, L. G.; Mayo, P. R.; Cass, G. R. *Characterization and Evolution of Primary and Secondary Aerosols During PM$_{2.5}$ and PM$_{10}$ Episodes in the South Coast Air Basin*; Final Report to Coordinating Research Council A-22; California Institute of Technology: 2000.
(28) Pastor, S. H.; Prather, K. A. *Refinement, Calibration, and Field Studies Involving Transportable Aerosol Time-of-Flight Mass Spectrometers*; Final Report to California Air Resources Board 96-307; University of California, Riverside: 2002.
(29) Allen, J. O.; Hughes, L. S.; Salmon, L. G.; Mayo, P. R.; Johnson, R. J.; Cass, G. R. *Atmos. Environ.* **2002**, submitted for publication.
(30) Hughes, L. S.; Allen, J. O.; Salmon, L. G.; Mayo, P. R.; Johnson, R. J.; Cass, G. R. *Environ. Sci. Technol.* **2002**, *36*, 3928−3935.
(31) Prather, K. A.; Nordmeyer, T.; Salt, K. *Anal. Chem.* **1994**, *66*, 1403−1407.
(32) Nordmeyer, T.; Prather, K. A. *Anal. Chem.* **1994**, *66*, 3540−3542.
(33) Gard, E.; Mayer, J. E.; Morrical, B. D.; Dienes, T.; Fergenson, D. P.; Prather, K. A. *Anal. Chem.* **1997**, *69*, 4083−4091.
(34) Marple, V. A.; Rubow, K. L.; Behm, S. M. *Aerosol Sci. Technol.* **1991**, *14*, 434−446.
(35) Wall, S. M.; John, W.; Ondo, J. L. *Atmos. Environ.* **1988**, *22*, 1649−1656.
(36) Mulik, J.; Puckett, R.; Willims, D.; Sawicki, E. *Anal. Lett.* **1976**, *9*, 653−663.
(37) Bolleter, W. T.; Bushman, C. T.; Tidwell, P. W. *Anal. Chem.* **1961**, *33*, 592−594.
(38) Silva, P. J.; Prather, K. A. *Anal. Chem.* **2000**, *72*, 3553−3562.
(39) Silva, P. J. Ph.D. Dissertation, University of California, Riverside, 2000.
(40) Angelino, S.; Suess, D. T.; Prather, K. A. *Environ. Sci. Technol.* **2001**, *35*, 3130−3138.
(41) Allen, J. O. *YAADA Reference Manual. Software Toolkit to Analyze Single-Particle Mass Spectral Data*; Arizona State University: 2001; http://www.yaada.org.
(42) Reents, W. D.; Downey, S. W.; Emerson, A. B.; Mujsce, A. M.; Muller, A. J.; Siconolfi, D. J.; Sinclair, J. D.; Swanson, A. G. *Plasma Sources Sci. Technol.* **1994**, *3*, 369−372.
(43) Morrical, B. D. Ph.D. Dissertation, University of California, Riverside, 1999.
(44) Carson, P. G.; Johnston, M. V.; Wexler, A. S. *Aerosol Sci. Technol.* **1997**, *26*, 291−300.

(45) Kleeman, M. J.; Hughes, L. S.; Allen, J. O.; Cass, G. R. *Environ. Sci. Technol.* **1999**, *33*, 4331−4341.

(46) Otten, Ph.; Bruynseels, F.; Van Grieken, R. *Anal. Chim. Acta* **1987**, *195*, 117−124.

(47) Stelson, A. W.; Seinfeld, J. H. *Atmos. Environ.* **1982**, *16*, 983−992.

(48) Wang, H.-C.; John, W. *Aerosol Sci. Technol.* **1988**, *8*, 157−172.

(49) Salt, K.; Noble, C. A.; Prather, K. A. *Anal. Chem.* **1996**, *68*, 230−234.